Oriented attachment and exchange coupling of α-Fe_2O_3 nanoparticles

C. Frandsen,[1,2] C. R. H. Bahl,[1,3] B. Lebech,[3] K. Lefmann,[3] L. Theil Kuhn,[3] L. Keller,[4] N. H. Andersen,[3] M. v. Zimmermann,[5] E. Johnson,[3,6] S. N. Klausen,[3,7] and S. Mørup[1]

[1]*Department of Physics, Technical University of Denmark, DK-2800 Kgs. Lyngby, Denmark*

[2]*School of Conservation, DK-1263 Copenhagen K, Denmark*

[3]*Materials Research Department, Risø National Laboratory, DK-4000 Roskilde, Denmark*

[4]*Laboratory for Neutron Scattering, ETHZ & PSI, CH-5232 Villigen PSI, Switzerland*

[5]*Hamburger Synchrotronstrahlungslabor HASYLAB at Deutsches Elektronen-Synchrotron DESY, D-22603 Hamburg, Germany*

[6]*Nano Science Center, Niels Bohr Institute, University of Copenhagen, DK-2100 Copenhagen Ø, Denmark*

[7]*Materials Science Division, Argonne National Laboratory, Argonne, Illinois 60439, USA*

(Received 17 July 2004; published 6 December 2005)

We show that antiferromagnetic nanoparticles of α-Fe_2O_3 (hematite) under wet conditions can attach into chains along a common [001] axis. Electron microscopy shows that such chains typically consist of two to five particles. X-ray and neutron diffraction studies show that both structural and magnetic correlations exist across the interfaces along the [001] direction. This gives direct evidence for exchange coupling between particles. Exchange coupling between nanoparticles can suppress superparamagnetic relaxation and it may play a role for attachment along preferred directions. The relations between exchange coupling, magnetic properties, and oriented attachment are discussed.

DOI: 10.1103/PhysRevB.72.214406 PACS number(s): 75.50.Tt, 61.46.+w, 68.35.Ct, 75.25.+z

I. INTRODUCTION

The magnetic properties of nanoparticles can be strongly influenced by interparticle interactions. For ferro- and ferrimagnetic nanoparticles, strong dipole interactions may result in a divergence of the superparamagnetic relaxation time at a finite temperature, which depends on the strength of the interactions.[1,2] Below this critical temperature, such samples may have many similarities to spin glasses.[2–6] The superparamagnetic relaxation of antiferromagnetic nanoparticles can also be significantly suppressed by interparticle interactions. In this case, the dipole interactions are too weak to explain the observed effects, and therefore it has been concluded that exchange interactions between surface atoms of particles in close proximity are responsible for the effects.[7–9] It has been shown that exchange interactions between ferromagnetic nanoparticles and an antiferromagnetic environment can result in a greatly enhanced magnetic anisotropy, and this may be utilized to increase the information density in magnetic recording media.[10] The exchange interaction depends crucially on the atomic arrangement at the interface between neighboring particles, and studies of the magnetic properties of interacting antiferromagnetic nanoparticles may therefore give new information about the way they attach. Currently there is considerable interest in understanding and controlling the arrangement of nanoparticles because it is of importance for a number of interesting phenomena, including revealing the mechanisms behind crystal growth[11–14] and developing new technologies for building up nanostructured devices.[15] In order to control positioning of magnetic nanoparticles, their magnetic dipole moments have been utilized to guide them in applied fields or in stray fields from neighboring particles.[16–20] Another potential method of controlling the position and properties of magnetic nanoparticles is to utilize exchange interaction between particles. Although this kind of interaction is rather unexplored, it holds interesting prospects. Exchange coupling between particles can be orders of magnitude larger than the dipole coupling if the particles are in close proximity. However, it is considered a major challenge to establish strong exchange coupling between nanoparticles.[21]

To examine the exchange coupling between particles it is fruitful to study particles of antiferromagnetic materials, because they have insignificant magnetic dipole interactions. The most abundant antiferromagnetic material is probably α-Fe_2O_3 (hematite).[22] It is the most stable form of iron oxide and commonly found in rocks and sediments on Earth and recently also on Mars.[23] It has a pseudohexagonal unit cell with six puckered Fe-layers perpendicular to the [001] direction and the spins of adjacent Fe-layers are coupled antiparallel.[22,24] In α-Fe_2O_3 nanoparticles the spins are confined to lie in the low anisotropy (001) plane.[25,26] Within this plane, the sublattice magnetization directions can easily rotate while rotation out of the plane requires much more energy. Therefore, superparamagnetic relaxation mainly takes place within the (001) plane.[26,27] Mössbauer spectroscopy studies have shown that the superparamagnetic relaxation can be suppressed in samples in which α-Fe_2O_3 nanoparticles have agglomerated, suggesting that strong exchange interaction exists between the particles.[7,9] However, no direct observation of the coupling has been reported so far. In the following, we present studies of nanoparticles of α-Fe_2O_3 using high-resolution electron microscopy, high-energy synchrotron x-ray diffraction, neutron powder diffraction, and Mössbauer spectroscopy. We find that α-Fe_2O_3 nanoparticles arrange into chains along a common [001] axis, and we directly observe that also the magnetic order continues across the interfaces in this direction.

II. EXPERIMENTAL DETAILS

We prepared α-Fe_2O_3 nanoparticles by a gel-sol method similar to that described by Sugimoto *et al.*[28] After formation

of the particles in an aqueous solution, excess ions were washed out and the particles were freeze-dried. In the following, this dried sample is referred to as the as-prepared sample. In order to study how the interactions may be diminished due to mechanical treatments the agglomerated α-Fe_2O_3 particles were ground together with nonmagnetic nanoparticles of amorphous SiO_2 (weight ratio 1:3) in air in an agate ball mill. The mill rotated gently, 40 times per minute for 2 days. The weight ratio between balls and sample was 15:1. Mössbauer spectroscopy and x-ray diffraction showed that no chemical reaction (less than 5 wt %, if any) took place during grinding.

High-resolution electron microscopy (HREM) images were obtained by means of a JEOL 3000F FEG transmission electron microscope (TEM) using lacey carbon film on 200 μm mesh Cu grids as sample supports. Cryo-TEM imaging was made with a Philips CM200 FEG TEM using an Oxford Instruments CT3500 cryoholder at liquid nitrogen temperature.

High-energy synchrotron x-ray diffraction (HES-XRD) data were obtained using the three-crystal diffractometer at the BW5 beam-line at HASYLAB at DESY in Germany with incident photons with a wavelength of 0.12513 Å (approximately 100 keV). The monochromator and analyzer systems consist of Si(111)/Ge gradient crystals giving a full width at half maximum (FWHM) instrumental resolution $B_{i,XRD}$ (approximately independent of scattering vector Q) that is 0.0135 $Å^{-1}$ at $Q=3.1$ $Å^{-1}$.

Neutron powder diffraction (NPD) data were collected by means of the DMC diffractometer placed at the neutron spallation source SINQ at the Paul Scherrer Institute in Switzerland. A wavelength of 4.20 Å was used. The instrumental resolution $B_{i,NPD}$ is 0.017 $Å^{-1}$ at $Q=1.37$ $Å^{-1}$ increasing to 0.020 $Å^{-1}$ at $Q=2.32$ $Å^{-1}$.

^{57}Fe Mössbauer spectra were obtained by use of a conventional constant acceleration Mössbauer spectrometer with a 50 mCi source of ^{57}Co in a rhodium matrix. Low-temperature spectra were obtained using a temperature-controlled liquid nitrogen cryostat. The spectrometers were calibrated with a 12.5 μm α-Fe foil at room temperature.

III. RESULTS AND ANALYSIS

A. Electron microscopy

High-resolution electron microscopy images of agglomerates of the particles from the as-prepared sample, dried on a grid, are shown in Figs. 1(a) and 1(b). The individual particles are typically 5–10 nm in diameter and have rounded shapes without pronounced facets. Noticeably, the micrographs show that neighboring particles have a tendency to be aligned along their common [001] axis. Since no (00l) planes are seen due to extinction, the orientation of the [001] axis of the particles can only be established from other planes identified from their planar spacings and mutual angles. Typically, chains of two to five particles are observed. In most cases, where the particles share a common [001] axis, the arrangement of particles appears epitaxial, i.e., the lattice planes are continued from one particle into its neighbor [Fig. 1(a)]. In one case we found that the lattice planes other than

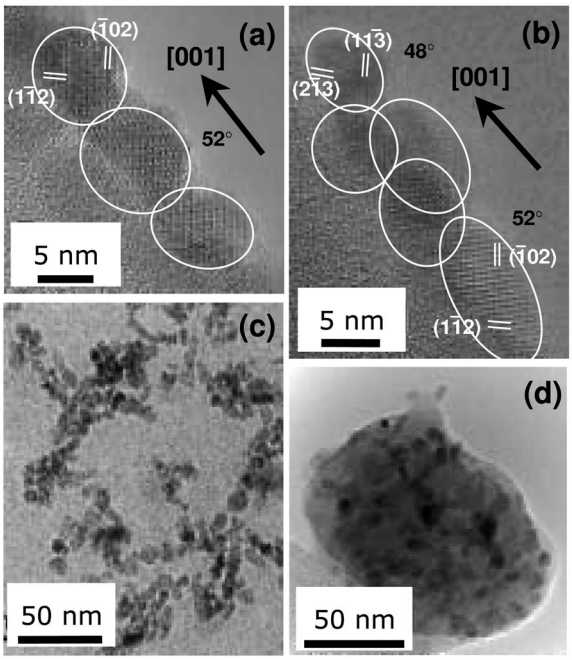

FIG. 1. Transmission electron microscopy images of α-Fe_2O_3 nanoparticles. (a), (b) HREM images showing that the particles are attached to one another along their common [001] axis. The arrows and angles indicate the direction of the [001] axis of the particles relative to the plane of the paper. The arrows point into the paper. (c) Cryo-TEM image of a frozen aqueous suspension of the particles. (d) Electron micrograph of the separated α-Fe_2O_3 particles (dark spots) after grinding with amorphous SiO_2 particles (the gray matrix of the composite).

(001) were not parallel for the first and the last particles in a chain [Fig. 1(b)], indicating that defects or polytypic stacking in principle could be incorporated by the attachment of the particles as suggested in Ref. 11. In general, polytypic stacking is difficult to observe by electron microscopy because the lattice planes of neighboring particles will only rarely be oriented parallel to the beam. Electron micrographs of a frozen aqueous suspension (cryo-TEM) show that the oriented particle arrangement is not induced by the substrate since the chain formation also is prevalent in suspension [Fig. 1(c)]. The TEM image, Fig. 1(d), shows that the α -Fe_2O_3 particles are rather well separated after grinding with amorphous silica.

B. X-ray diffraction

A quantitative measure of the correlation lengths associated with the attached particles can be obtained from diffraction data because the correlation lengths can be assumed to be inversely proportional to the broadening of the diffraction lines.[29] Figure 2(a) shows high-energy synchrotron x-ray diffraction data for the as-prepared sample. Most of the observed peaks correspond to the reflections expected for α-Fe_2O_3, but they are considerably broadened. Two narrow and resolution-limited peaks are the (200) aluminium reflection at 3.096 $Å^{-1}$ and a weak spurious peak of unidentified origin at 1.513 $Å^{-1}$. The observed Bragg peaks in the high-energy

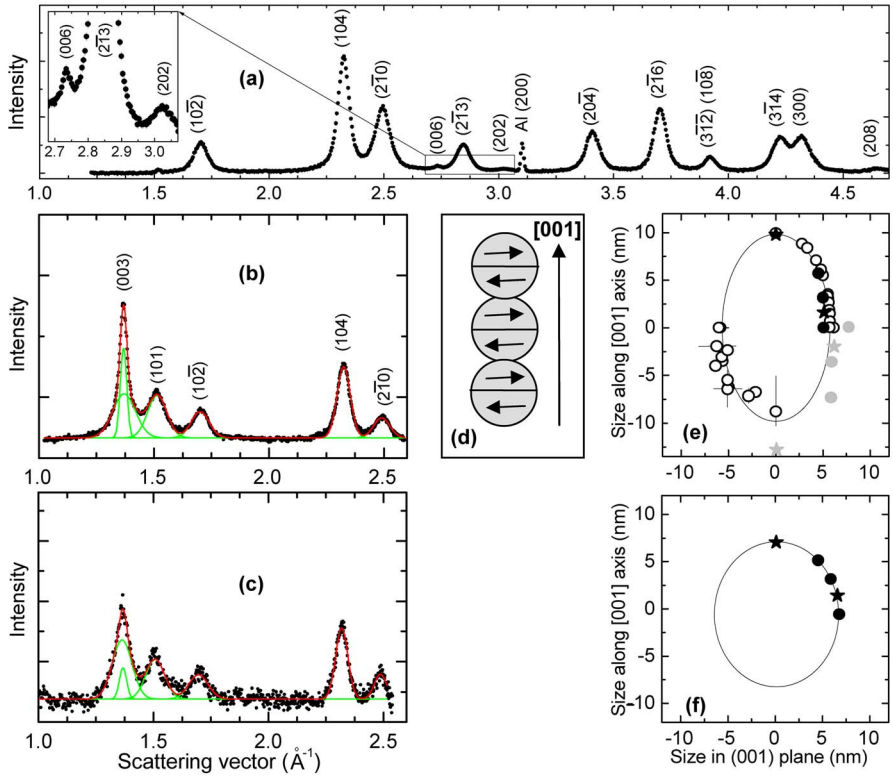

FIG. 2. (Color online) Diffraction data (background subtracted) of α-Fe_2O_3 particles obtained at room temperature. (a) HES-XRD data of the as-prepared nanoparticles. (b) NPD data of the same sample as in (a). (c) NPD data of the α-Fe_2O_3 sample after grinding. In (b) and (c), the solid lines represent the fits with Gaussian shaped peak profiles to the data (green denotes individual peaks, red the sum of peaks). (d) Schematic illustration of the antiferromagnetic correlation across the particle interfaces in the as-prepared sample. (e) Correlation lengths obtained for the as-prepared sample from HES-XRD (open dots) and NPD (filled dots) data by Fullprof fitting (first quadrant), and by fitting with pseudo-Voigt (third quadrant) and Gaussian (fourth quadrant, gray) peak profiles. Stars denote magnetic reflections. (f) Correlation lengths from Fullprof fitting for the ground sample, based on NPD data. The ellipses in (e) and (f) are guides to the eye obtained from the Fullprof fit.

synchrotron x-ray data were fitted to Gaussian shaped peak profiles. The crystalline correlation length, estimated from the FWHM of the α-Fe_2O_3 reflections as $2\pi/(\mathrm{FWHM}^2\text{-}B_{i,XRD}{}^2)^{1/2}$, was found to be typically about 7–8 nm. This correlation length is similar to the average particle size found by HREM. The (006) reflection is narrower and the correlation length was found to be longest along [001], indicating that the crystalline correlation exceeds the particle size in that direction. However, since the (006) peak is weak and partly overlapping with the much more intense (2$\bar{1}$3) reflection, the estimated width of the (006) reflection depends on the choice of peak profile and the background estimate. Therefore, the correlation length in the [001] direction as determined from the (006) reflection is only indicative of extended particle alignment in the [001] direction.

C. Neutron diffraction

While x-ray diffraction provides information solely about the crystalline structure, neutron diffraction also reveals magnetic correlations. Figures 2(b) and 2(c) show neutron powder diffraction data for the as-prepared and the ground samples, respectively. These patterns also show broadened Bragg reflections when compared to the resolution-limited Gaussian diffraction peaks from a powder sample of α-Fe_2O_3 with grain size in the micrometer range.

The (003) and (101) reflections are purely magnetic; the remaining reflections are structural. In the spectrum of the as-prepared sample, most of the diffraction peaks have widths in accordance with the correlation length derived from the x-ray data. However, it is noticeable that the antiferromagnetic (003) reflection is considerably narrower than other reflections. This shows directly that the crystallographic alignment along [001] is accompanied by a similar magnetic correlation in that direction. The strong magnetic (003) reflection, which allows for a more detailed analysis than the weak structural (006) reflection, can be modeled by two Gaussian shaped contributions. After correction for the experimental resolution, one of these has a width corresponding to the average particle size, while the other, which covers ~36% of the total (003) reflection area, has a width corresponding to 22 nm. This suggests that on average about one-third of the particles have magnetic correlations extending over about three particle diameters along the [001] direction as illustrated schematically in Fig. 2(d).

The neutron diffraction data of the ground sample (after subtracting the contribution of the ground SiO_2 particles),

displayed in Fig. 2(c), show that after grinding, all reflections have widths almost corresponding to the size of the individual nanoparticles with nearly spherical shape. Thus the grinding has to a large extent destroyed the magnetic and structural correlation of neighboring particles without reducing the particle size. A double peak analysis of the ground sample results in a small narrow contribution to the (003) reflection, indicating that some of the particles may remain aligned after grinding.

A traditional way of analyzing powder diffraction data is by profile refinement. Therefore, in addition to modeling the data according to the description illustrated in Fig. 2(d), we have also analyzed the x-ray and neutron diffraction data by means of the refinement program FULLPROF,[30] which has the possibility to include anisotropic size broadening of the observed diffraction peaks. The analysis was based on the assumption that the chains of attached particles could be described as ellipsoidal-shaped particles. For the as-prepared sample this analysis showed average correlation lengths of ~10 nm and ~6 nm parallel and perpendicular to the [001] direction, respectively. The average correlation length in the [001] direction agrees within experimental accuracy with the average correlation length of ~13 nm estimated from the double peak analysis of the (003) reflection of the as-prepared sample. In contrast, the ground sample showed average correlation lengths of ~7 nm both parallel and perpendicular to the [001] direction. Hence, the FULLPROF analysis supports the conclusion of particle alignment along the [001] direction in the as-prepared sample.

FULLPROF fitting includes shape constraints as well as crystallographic constraints obtained for bulk materials, which determine the intensities, and which may not adapt to nanoparticles. Therefore, we have also fitted the diffraction peaks with pseudo-Voigt profiles without such constraints. This resulted in correlation lengths, which within the error bars are identical to those obtained from FULLPROF fitting.

Figures 2(e) and 2(f) show the correlations lengths for the different crystallographic directions obtained from the different types of fits of the as-prepared sample and the ground sample, respectively. For the as-prepared sample, all fits show that the correlation is longest along the [001] direction, while for the ground sample the correlation lengths are almost identical in all crystallographic directions. The directions closest to the [001] direction in the as-prepared sample have longer correlation lengths than those within the [001] plane. This supports the theory that the attachment of the particles is primarily epitaxial. In the case of polytypic particle arrangement along the [001] axis, only the [001] correlation length would be long and, e.g., the [104] correlation length would be similar to the in-plane correlation length, but this is not found. It is possible that during the epitaxial attachment of the particles the order of the six Fe-layers in the unit cell is not continued across the grain boundaries [this is equivalent to formation of stacking faults or twinning of (001) planes at the interfaces]. However, the data do not allow for a quantitative analysis of how prevalent such stacking might be.

Strain may, like nanocrystallinity, lead to broadening of the diffraction peaks. The diffraction data in Fig. 2 have only a couple of reflections belonging to the same directions in the crystal structure; therefore, we were not able to perform a full Williamson-Hall analysis of the strain in the various directions. However, the available data as well as previous studies of α-Fe_2O_3 nanoparticles prepared by the same technique[26,31] showed no significant influence of strain on the line broadening.

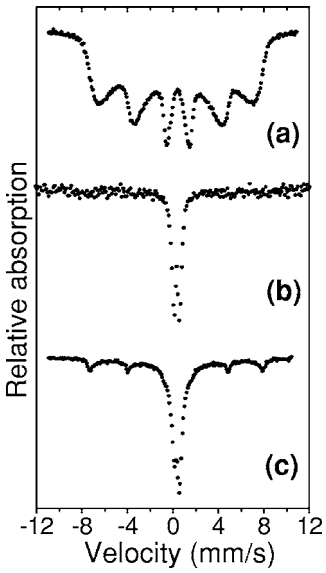

FIG. 3. Mössbauer spectra of α-Fe_2O_3 nanoparticles. (a) The as-prepared sample measured at ambient temperature. (b) The ground sample at ambient temperature. (c) The ground sample at 80 K.

The observation that both structural and magnetic correlations exceed the particle size in the [001] direction indicates that the distance between the (001) layers is the same across the interface as inside the particles. The constant separation of the (001) layers across the interface indicates that the surface layer of water or hydroxyl groups, which typically are adsorbed to nanoparticles, is expelled from the interface. The attachment of particles, with interfaces having more or less the same structure and chemical bonds as inside the crystals, is expected to result in relatively strong mechanical coupling between the particles.

The magnetic correlation along [001] shows that the alternating magnetization directions of the (001) layers of the particles are continued across the particle interfaces as illustrated in Fig. 2(d). The sublattice magnetization directions are arranged within the (001) planes such that the antiferromagnetic order is continued across the interface. The correlation implies that the exchange coupling exists across the interfaces and is similar to the exchange coupling between the Fe-layers within the particles. This is direct evidence of strong exchange coupling between particles.

D. Mössbauer spectroscopy

By use of Mössbauer spectroscopy we have studied the influence of sample treatments on interactions via studies of the superparamagnetic relaxation of the particles. The Mössbauer spectrum of the as-prepared sample, obtained at room temperature [Fig. 3(a)], consists of a sextet with broadened

lines, typical for samples of interacting nanoparticles.[7,9,32] There is no fast superparamagnetic relaxation in this sample, as indicated from the absence of a central doublet. After grinding the as-prepared sample, the room temperature spectrum, shown in Fig. 3(b), contains only a doublet. This indicates that all the particles now have fast superparamagnetic relaxation at this temperature. The doublet dominates down to at least 80 K [Fig. 3(c)]. The superparamagnetic blocking temperature was found to be about 50 K. This shows that the grinding has led to a significant reduction of the interactions such that the ground particles exhibit fast superparamagnetic relaxation in accordance with previous studies of the influence of grinding of interacting nanoparticles.[31]

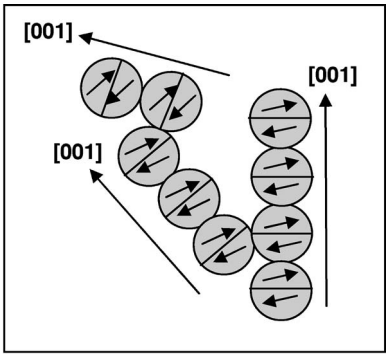

FIG. 4. Illustration of network of interacting α-Fe_2O_3 nanoparticles showing suppressed superparamagnetic relaxation at room temperature.

IV. DISCUSSION

Our results from electron microscopy and diffraction measurements show that on average a third of the particles in the as-prepared sample are attached into chains of three particles along a common [001] axis such that there is both structural and magnetic correlation in that direction. Gentle grinding can lead to separation of particles and reduce the correlation along [001]. Mössbauer studies show that superparamagnetic relaxation is suppressed even at room temperature in the as-prepared sample, but separation of particles by grinding leads to fast superparamagnetic relaxation.

Previous studies have shown that the only possible explanation for the strong suppression of superparamagnetic relaxation in the samples of agglomerated α-Fe_2O_3 nanoparticles is interparticle exchange interaction.[7,9] The magnetic correlation extending over several particles found in the present work is, however, a direct observation of exchange coupling existing between the particles.

In order to fully explain the suppression of superparamagnetic relaxation observed even at room temperature for all particles in the as-prepared sample, it is insufficient to consider solely interparticle exchange coupling for the fraction of the particles aligned into chains of about three particles. This would at maximum raise the blocking temperature by a factor of about 3 for about a third of the particles. Recent studies show that α-Fe_2O_3 nanoparticles may also agglomerate in a more random fashion during drying, i.e., with nonparallel [001] axes, but exchange coupling still exists across the interfaces [seen as a slight rotation of the sublattice magnetization out of the (001) plane],[33] although the coupling between particles with nonparallel [001] axes is likely to be weaker than between particles with parallel [001] axes.

The strong suppression of superparamagnetic relaxation in samples of agglomerated particles therefore seems to be due to the existence of larger networks of interacting particles with both parallel and nonparallel [001] axes. Figure 4 shows a schematic illustration of such a network. Here the particles are attached into small chains with parallel [001] axes, but the neighboring chains or particles have different orientations of their [001] axes. The picture of the magnetic structure and dynamics of particles as being governed by a network of exchange coupled, aligned and nonaligned particles is in good agreement with the model proposed in Ref. 7. In this model, it was assumed, in order to explain Mössbauer data of interacting 20 nm α-Fe_2O_3 particles, that the easy axes of the particles were parallel to the effective exchange field. This described most of the features well. Other features, which this model could not describe, were ascribed to interacting particles with nonparallel easy axes. Here we have obtained more direct observations of the arrangement and magnetic coupling of the particles assumed by the model.

It is interesting that oriented attachment is achieved between antiferromagnetic nanoparticles of α-Fe_2O_3 when prepared by wet chemistry or when dried from aqueous suspensions. Until recently, the general understanding was that crystals grow by addition of ions, but studies of TiO_2 and iron oxyhydroxides have lately revealed that crystals can also grow by oriented attachment of nanoparticles.[11–14] Particles in suspension may be brought together by Brownian motion, whereupon strong short-range forces cause the attachment. It has been suggested that reduction of surface energy of nanoparticles is the driving mechanism for this type of crystal growth.[11–14] The oriented attachment of the α-Fe_2O_3 nanoparticles with parallel [001] directions is surprising because the particles are nominally equidimensional[34] and the (001) planes of α-Fe_2O_3 are generally considered to be the planes of low surface energy. Calculations have shown that the (001) surface energy of α-Fe_2O_3 takes values between 0.75 and 1.65 J/m^2 depending on the environment.[35,36] Hydration as well as oxygen vs iron termination can significantly alter the surface energies.[35,36] Since α-Fe_2O_3 is magnetic and since we observe exchange coupling between agglomerated particles, it is worth considering if exchange interaction between particles can affect the attachment. As an example, we look at the interactions at the (001) interface. Magnetic coupling mechanisms would make it favorable for the particles to attach with parallel (001) planes: the superexchange coupling across the oxygen-layers is dominant compared to in-plane exchange interaction,[22] and the (001) plane is the plane where all spins are parallel so that coupling of two (001) planes will lead to least spin frustration. We find the exchange interaction between (001) planes to be 0.2 J/m^2 by using that the density of Fe-atoms in the (001) plane is one Fe per 11×10^{-20} m^2 and the exchange energy density is 2×10^{-20} J per Fe-atom (the energy density is calculated from the experimentally found ex-

change coupling constants, J_3 and J_4, of Ref. 37; an overview of the different types of exchange couplings within α-Fe_2O_3 is found in Ref. 22). Since the exchange energy is comparable in size, although smaller, to the surface energy, the contribution from the exchange energy may thus be considered an extra driving force for the oriented attachment. Exchange interactions between particles with non-parallel (001) planes may lead to magnetic frustration, which could result in repulsive forces.

V. CONCLUSIONS

The present study shows that α-Fe_2O_3 nanoparticles may show oriented attachment such that both the crystallographic and the magnetic correlations continue across the interfaces. The nanoscale coupling between particles is found to be sensitive to macroscopic handling such as gentle grinding. The observed alignment of α-Fe_2O_3 nanoparticles along a common [001] axis can in part explain the strong exchange coupling between agglomerated α-Fe_2O_3 particles, observed by Mössbauer spectroscopy as a suppression of the superparamagnetic relaxation. A complete description of the magnetic properties of the agglomerated particles can be obtained by also taking into account exchange coupling between particles with nonparallel [001] axes. It is possible that exchange coupling between nanoparticles plays a driving role for the arrangement of the particles. Studies of the mechanisms of exchange coupling and oriented attachment between nanoparticles are important for the understanding of crystal growth, and for the magnetic and the mechanical properties of, e.g., sediments formed under different conditions in nature, as well as for designing exchange coupled nanocrystalline magnetic materials and nanoscale devices.

ACKNOWLEDGMENTS

We thank Haldor Topsøe A/S, Kgs. Lyngby, Denmark, for the use of their cryo-TEM equipment. We acknowledge beam time allocation at Swiss Spallation Neutron Source, Paul Scherrer Institute SINQ, Villigen, Switzerland, and at Hamburger Synchrotronstrahlungslabor HASYLAB at Deutsches Elektronen-Synchrotron DESY, D-22603 Hamburg, Germany. The work was supported by the Danish Technical Research Council through the nanomagnetism framework programme and the Danish Natural Science Research Council through DANSCATT and Dansync.

[1] J. Zhang, C. Boyd, and W. Luo, Phys. Rev. Lett. **77**, 390 (1996).
[2] C. Djurberg, P. Svedlindh, P. Nordblad, M. F. Hansen, F. Bødker, and S. Mørup, Phys. Rev. Lett. **79**, 5154 (1997).
[3] H. Mamiya, I. Nakatani, and T. Furubayashi, Phys. Rev. Lett. **80**, 177 (1998).
[4] D. Fiorani, J. L. Dormann, R. Cherkaoui, E. Tronc, F. Lucari, F. D'Orazio, L. Spinu, M. Nogues, A. Garcia, and A. M. Testa, J. Magn. Magn. Mater. **196-197**, 143 (1999).
[5] T. Jonsson, P. Svedlindh, and M. F. Hansen, Phys. Rev. Lett. **81**, 3976 (1998).
[6] Y. Sun, M. B. Salamon, K. Garnier, and R. S. Averback, Phys. Rev. Lett. **91**, 167206 (2003).
[7] M. F. Hansen, C. B. Koch, and S. Mørup, Phys. Rev. B **62**, 1124 (2000).
[8] F. Bødker, M. F. Hansen, C. B. Koch, and S. Mørup, J. Magn. Magn. Mater. **221**, 32 (2000).
[9] C. Frandsen and S. Mørup, J. Magn. Magn. Mater. **266**, 36 (2003).
[10] V. Skumryev, S. Stoyanov, Y. Zhang, G. Hadjipanayis, D. Givord, and J. Noqués, Nature (London) **423**, 850 (2003).
[11] R. Lee Penn and J. F. Banfield, Science **281**, 969 (1998).
[12] R. Lee Penn and J. F. Banfield, Geochim. Cosmochim. Acta **63**, 1549 (1999).
[13] J. F. Banfield, S. A. Welch, H. Zhang, T. T. Ebert, and R. Lee Penn, Science **289**, 751 (2000).
[14] M. Nesterova, J. Moreau, and J. F. Banfield, Geochim. Cosmochim. Acta **67**, 1177 (2003).
[15] P. M. Mendes, Y. Chen, R. E. Palmer, K. Nikitin, D. Fitzmaurice, and J. A. Preece, J. Phys.: Condens. Matter **15**, S3047 (2003).
[16] K. Butter, P. H. H. Bomans, P. M. Frederik, G. J. Vroege, and A. P. Philipse, Nat. Mater. **2**, 88 (2003).
[17] Y. Lalatonne, J. Richardi, and M. P. Pileni, Nat. Mater. **3**, 121 (2004).
[18] A. Ghazali and J.-C. Lévy, Phys. Rev. B **67**, 064409 (2003).
[19] V. F. Puntes, K. M. Krishnan, and A. P. Alivisatos, Science **291**, 2115 (2001).
[20] V. F. Puntes, P. Gorostiza, D. M. Aruguete, N. G. Bastus, and A. P. Alivisatos, Nat. Mater. **3**, 263 (2004).
[21] H. Zeng, J. Li, Z. L. Wang, and S. Sun, Nature **420**, 395 (2002).
[22] A. H. Morrish, *Canted Antiferromagnetism: Hematite* (World Scientific, Singapore, 1994).
[23] P. R. Christensen, J. L. Bandfield, R. N. Clark, K. S. Edgett, V. E. Hamilton, T. Hoefen, H. H. Kieffer, R. O. Kuzmin, M. D. Lane, M. C. Malin, R. V. Morris, J. C. Pearl, R. Pearson, T. L. Roush, S. W. Ruff, and M. D. Smith, J. Geophys. Res., [Planets] **105**, 9623 (2000); R. V. Morris, G. Klingelhöfer, B. Bernhardt, C. Schröder, D. S. Rodionov, P. A. de Souza, A. Yen, R. Gellert, E. N. Evlanov, J. Foh, E. Kankeleit, P. Gütlich, D. W. Ming, F. Renz, T. Wdowiak, S. W. Squyres, and R. E. Arvidson, Science **305**, 833 (2004); G. Klingelhöfer, R. V. Morris, B. Bernhardt, C. Schröder, D. S. Rodionov, P. A. de Souza, A. Yen, R. Gellert, E. N. Evlanov, B. Zubkov, J. Foh, U. Bonnes, E. Kankeleit, P. Gütlich, D. W. Ming, F. Renz, T. Wdowiak, S. W. Squyres, and R. E. Arvidson, *ibid.* **306**, 1740 (2004).
[24] C. G. Shull, W. A. Stauser, and E. O. Wollan, Phys. Rev. **83**, 333 (1951).
[25] W. Kündig, H. Bömmel, G. Constabaris, and R. H. Lindquist, Phys. Rev. **142**, 327 (1966).
[26] F. Bødker and S. Mørup, Europhys. Lett. **52**, 217 (2000).
[27] F. Bødker, M. F. Hansen, C. B. Koch, K. Lefmann, and S. Mørup, Phys. Rev. B **61**, 6826 (2000).
[28] T. Sugimoto, Y. Wang, H. Itoh, and A. Muramatsu, Colloids Surf., A **134**, 265 (1998).
[29] B. E. Warren, *X-ray Diffraction* (Dover, New York, 1990).

[30] J. Rodriguez-Carvajal, Physica B **192**, 55 (1993).
[31] M. Xu, C. R. H. Bahl, C. Frandsen, and S. Mørup, J. Colloid Interface Sci. **279**, 132 (2004).
[32] S. Mørup, C. Frandsen, F. Bødker, S. N. Klausen, K. Lefmann, P.-A. Lindgård, and M. F. Hansen, Hyperfine Interact. **144/145**, 347 (2002).
[33] C. Frandsen and S. Mørup, Phys. Rev. Lett. **94**, 027202 (2005).
[34] R. Lee Penn, G. Oskam, T. J. Strathmann, P. C. Searson, A. T. Stone, and D. R. Veblen, J. Phys. Chem. B **105**, 2177 (2001).
[35] F. Jones, A. L. Rohl, J. B. Farrow, and W. van Bronswijk, Phys. Chem. Chem. Phys. **2**, 3209 (2000).
[36] X.-G. Wang, W. Weiss, S. K. Shaikhutdinov, M. Ritter, M. Petersen, F. Wagner, R. Schlögl, and M. Scheffler, Phys. Rev. Lett. **81**, 1038 (1998).
[37] E. J. Samuelsen and G. Shirane, Phys. Status Solidi **42**, 241 (1970).